International Journal of Biological Macromolecules 242 (2023) 124621

Contents lists available at ScienceDirect

International Journal of Biological Macromolecules

journal homepage: www.elsevier.com/locate/ijbiomac

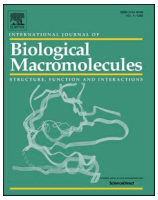

Amyloidogenic and non-amyloidogenic molten globule conformation of β-lactoglobulin in self-crowded regime

Sara Venturi [a], Barbara Rossi [b], Mariagrazia Tortora [b,c], Renato Torre [a,d], Andrea Lapini [a,e], Paolo Foggi [a,f,g], Marco Paolantoni [f,*], Sara Catalini [a,g,h,**]

[a] European Laboratory for Non-Linear Spectroscopy, Università di Firenze, Via Nello Carrara 1, 50019 Sesto Fiorentino, Italy
[b] Elettra-Sincrotrone Trieste, S.S. 114 km 163.5, Basovizza, 34149 Trieste, Italy
[c] AREA SCIENCE PARK, Padriciano, 99, 34149 Trieste, Italy
[d] Dipartimento di Fisica ed Astronomia, Università di Firenze, Via G. Sansone, 1, 50019 Sesto Fiorentino, Italy
[e] Dipartimento di Scienze Chimiche, della Vita e della Sostenibilità Ambientale, Università degli Studi di Parma, Parco Area delle Scienze, 17/A, 43124 Parma, PR, Italy
[f] Dipartimento di Chimica, Biologia e Biotecnologie, Università di Perugia, Via Elce di sotto 8, 06123 Perugia, Italy
[g] CNR-INO, Consiglio Nazionale Delle Ricerche – Istituto Nazionale di Ottica, Largo Fermi 6, 50125 Florence, Italy
[h] Dipartimento di Fisica e Geologia, Università di Perugia, 06123, Via Pascoli, Perugia, Italy

ARTICLE INFO

Keywords:
β-Lactoglobulin
Amyloid-aggregates
Self-crowding
UVRR
FTIR

ABSTRACT

Molecular insights on the β-lactoglobulin thermal unfolding and aggregation are derived from FTIR and UV Resonance Raman (UVRR) investigations. We propose an in situ and *in real-time* approach that thanks to the identification of specific spectroscopic markers can distinguish the two different unfolding pathways pursued by β-lactoglobulin during the conformational transition from the folded to the molten globule state, as triggered by the pH conditions. For both the investigated pH values (1.4 and 7.5) the greatest conformational variation of β-lactoglobulin occurs at 80 °C and a high degree of structural reversibility after cooling is observed. In acidic condition β-lactoglobulin exposes to the solvent its hydrophobic moieties in a much higher extent than in neutral solution, resulting on a highly open conformation. Moving from the diluted to the self-crowded regime, the solution pH and consequently the different molten globule conformation select the amyloid or non-amyloid aggregation pathway. At acidic condition the amyloid aggregates form during the heating cycle leading to the formation of transparent hydrogel. On the contrary, in neutral condition the amyloid aggregates never form. Information on the secondary structure conformational change of β-lactoglobulin and the formation of amyloid aggregates are obtained by FTIR spectroscopy and are related to the information of the structural changes localized around the aromatic amino acid sites by UVRR technique. Our results highlight a strong involvement of the chain portions where tryptophan is located on the formation of amyloid aggregates.

1. Introduction

Globular proteins are the most abundant proteins in nature, existing in a huge variety of three-dimensional structures. The conversion of soluble globular proteins into extended amyloid aggregates is one of the foundational causes for the onset of relevant amyloid pathologies [1]. However, amyloid aggregates are also found to play vital functional roles in different living organisms spanning from bacteria to human [2]. Moreover, some properties of amyloid aggregates such as their morphology, high mechanical strength, and chemical stability, to mention only a few, make them good candidates to fabricate new functional materials with emergent properties [3]. Indeed, the natural existence of protein amyloid aggregates that act as cellular self-defence systems and as highly engineered machines has been discovered [4,5], opening interesting perspectives for their application in material science field [4,5]. In this context, nanofibrillar aggregation might be exploited to develop specific protein hydrogels, as novel tuneable biomaterials [6]. Overall, a deep understanding of amyloid formation is of relevance in different fields other than medicine and cellular biology, such as for instance, tissue engineering, nanotechnology and food science [6–8].

The molecular mechanism responsible of the protein self-assembly is very complex, it involves the interplay of different types of interactions

* Corresponding author.
** Correspondence to: S. Catalini, European Laboratory for Non-Linear Spectroscopy, Università di Firenze, Via Nello Carrara 1, 50019 Sesto Fiorentino, Italy.
E-mail addresses: marco.paolantoni@unipg.it (M. Paolantoni), catalini@lens.unifi.it (S. Catalini).

https://doi.org/10.1016/j.ijbiomac.2023.124621
Received 5 September 2022; Received in revised form 16 April 2023; Accepted 23 April 2023
Available online 3 May 2023

and remains among the most puzzling problems in biophysics. The capability of forming amyloid aggregates, which are characterized by cross-β structures, is a rather general property of non-native proteins [5]. On the other hand, the amyloid aggregation pathways, which are protein-type dependent, can be differentiated by changing the experimental conditions (protein concentration, pH, temperature, or solvation properties) to select the final aggregation structuring. Often amyloid fibrils and protein hydrogels are produced in vitro starting from low concentrated protein samples (tens of mg/mL), with relatively long treatments (hours or days) at high temperatures and low pH [6,9]. In these conditions, fragments produced by hydrolytic processes often initiate the aggregation process. On the other hand, investigations on amyloid formation in concentrated samples have been more rarely accomplished, despite the importance of crowded and self-crowded protein systems in several areas, including cellular biology and pharmaceutics [10–13]. To fill the gap, in recent works [14–16] the heat-induced amyloid aggregation of the model protein lysozyme has been deeply investigated in self-crowded samples (>100 mg/mL) and acidic conditions. The aggregation process was monitored in situ and *in real-time* by spectroscopic approaches, demonstrating that amyloid oligomers develop quickly in denaturing conditions, leading to the formation of transparent thermoreversible hydrogels. These are constituted by interconnected (kinetically trapped) amyloid oligomers (not fibrils), which have a limited thermal stability and tend to dissociate at high temperatures. To note that amyloid oligomers are expected to be cytotoxic species with high reactivity [14–17] while amyloid fibrils are stable and less reactive products [17–19]. Recent studies indicate that the formation of reversible or irreversible aggregates depends on the conformations assumed by the proteins during the unfolding pathways [20].

Among globular proteins, β-lactoglobulin (β-Lg) reveals a strong propensity to aggregate [21], forming amyloid species with emergent properties [22]. β-Lg is a small globular protein present in the milk of most mammals and is the most abundant of the whey proteins (ca. 60 %). β-Lg boasts attractive functional qualities such as high solubility, emulsification capacity, strong viscosity, gelation propensity and foaming [23]. Moreover, it has high nutritional values and thus it is often used as additive in a wide number of food products [24]. Because of its high natural abundance, high nutritional value and interesting physicochemical properties, β-Lg is a promising candidate for several industrial large-scale applications. β-Lg has high bond affinity with hydrophobic nutrients and lipophilic drugs, typical of the lipocalin protein family [25]. It presents a strong resistance against digestion [26], making it a good acid-resistant carrier useful for the delivery of nutrients and pharmaceuticals in the gastrointestinal tract [24]. Recently, aerogels formed by amyloid fibrils of β-Lg evidence high conductivity and the capability to adsorbs organic pollutants from water, revealing interesting engineering applications for sensors [27,28] and water purification [29,30]. Many of the β-Lg interesting properties and its great versatility for the different applications are related to the hydrophobic cavity present in the structure, reported in Fig. S1 of the supporting material. β-Lg is composed by 162 amino acids, with a molecular weight of 18.4 kDa and an isoelectric point at pH 5.1. It has been subjected to several investigations concerning its structure and aggregation, demonstrating that different unfolding and aggregations pathways occur in different experimental conditions [8,9,21,31–36].

The present work aims at investigating heat-induced aggregation of amyloid-type in highly concentrated solutions of β-Lg (100 and 200 mg/mL) and at two pH values (1.4 and 7.5). The selected experimental conditions allowed us monitoring *in real-time* and in situ thermal-induced variations of the β-Lg conformation, as well as the formation of amyloid cross β-structure by Fourier transform infrared (FTIR) spectroscopy. Moreover, synchrotron-based Ultraviolet Resonance Raman (UVRR) spectroscopy was employed to probe local conformational variations around the aromatic amino acids [37,38] during the aggregation process. A comparative investigation of diluted β-Lg samples (20 mg/mL) was performed as a benchmark to evidence temperature-induced structural changes when aggregation processes can be neglected [14–16,39].

2. Experimental section

2.1. Samples preparation

The lyophilized powder of β-lactoglobulin from bovine milk (Sigma Aldrich, L0130-5G) is dissolved in deuterium oxide (99.9 atom % D, Sigma Aldrich), to prepare solutions with different protein concentration. Depending on the sensitivity of the used experimental techniques, the diluted protein samples are prepared with a content of 3.5 mg of protein/mL of solvent (here referred as mg/mL) and 20 mg/mL to perform UVRR and FTIR measurements, respectively. The concentrated samples reach a protein content of 100 mg/mL and 200 mg/mL. The protein total solubilisation is achieved by using a vortex mixer and subsequently the solution pH is adjusted with small amount of deuterium chloride (2 M), to reach final pH values of 1.4 and 7.5.

2.2. FTIR spectra

Infrared absorption measurements are collected using a FTIR Bruker spectrometer model Alpha. The software Opus 6.5 Bruker Optics is used for the acquisition of the spectra and the version 8.1 for their analysis. Spectra are performed using a homemade cell equipped with CaF_2 windows and optical path length is adjusted with Teflon spacers. After loading the sample between the windows, the cell is placed into a jacket whose temperature is controlled by a Peltier system. The spectra are acquired with a resolution of 2 cm^{-1}, by averaging 30 scans and analysed in the spectral range from 1750 to 1350 cm^{-1}. During the thermal ramp, before recording the spectrum, the sample is left to reach the set temperature for 5 min.

2.3. UVRR spectra

UV Resonance Raman (UVRR) experiments using synchrotron radiation (SR) are carried out at the BL10.2-IUVS beamline of Elettra Sincrotrone Trieste (Italy) [37]. The exciting wavelength is set at 226 nm by regulating the aperture of the undulator gap and using a Czerny-Turner monochromator (Acton SP2750, focal length 750 mm, Princeton Instruments, USA) equipped with a holographic grating with 3600 grooves/mm for monochromatizing the incoming SR. The UVRR spectra are collected in a back-scattered geometry by a single pass Czerny–Turner spectrometer of 750 mm focal length equipped with holographic grating with 1800 grooves/mm. The spectral resolution is set to about 2 cm^{-1}/pixel. The calibration of the spectrometer is standardized using cyclohexane (spectroscopic grade, Sigma Aldrich), which does not absorb UV within the wavelength range of interest. The UVRR spectra of protein solutions are collected in the amide region (1000–1700 cm^{-1}). During all the experiments the power radiation on the sample is kept low, about 24 μW, and the sample cell is continuously horizontally displaced during the measurements to avoid possible photodamage effects or heating of the sample. The Raman spectra of solutions are acquired at different values of temperature ranging from 25 °C to 95 °C using a sample holder equipped with a thermal bath coupled to a resistive heating system to keep the temperature of the sample at a fixed value with a stability of ±0.1 °C.

3. Results and discussion

3.1. β-Lg global conformation probed by FTIR spectroscopy

Fig. 1a–c shows the temperature dependence of FTIR spectra of the diluted and the concentrated β-Lg solution at pH 1.4, in the amide frequency region.

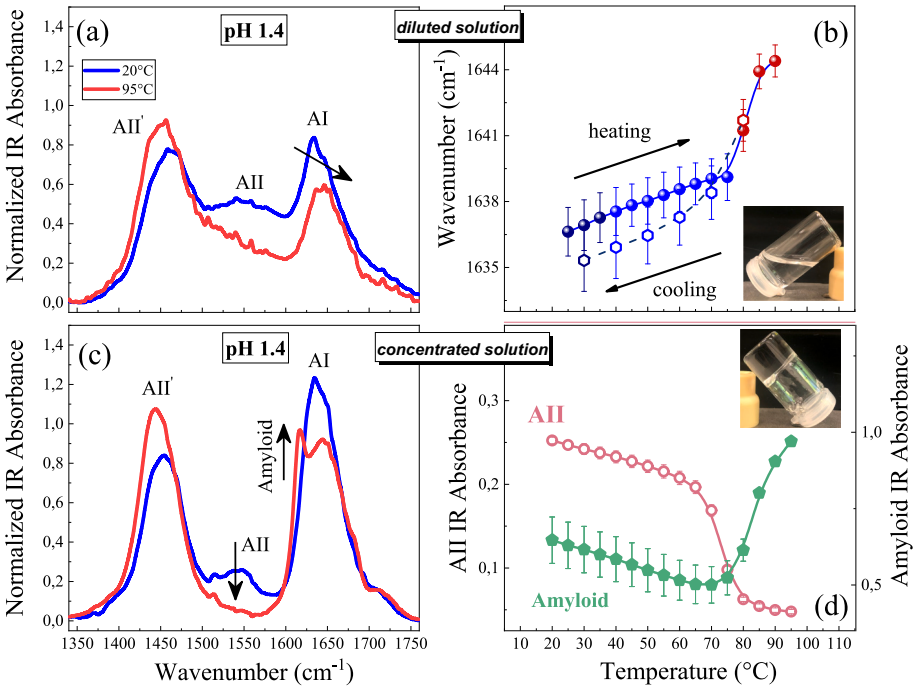

Fig. 1. Panels (a) and (c) show the FTIR spectra of β-Lg solutions at pH 1.4, recorded at 20 °C and at 95 °C, of the diluted (20 mg/mL) and of the concentrated (200 mg/ml) β-Lg solutions, respectively. Panel (b) reports the frequency centre of gravity of the AI signal during the heating and the cooling thermal treatments of the diluted β-Lg solution. Panel (d) displays the temperature dependence of IR absorbance of the AII (1550 cm^{-1}) and the amyloid (1617 cm^{-1}) signals for the concentrated β-Lg solution. After the heating cycle, the formation of a transparent hydrogel is observed for the concentrated solution of protein (see photo inside panel d).

The FTIR spectra of β-Lg reported in Fig. 1a,c show the amide II (AII) signal at 1550 cm^{-1} that is mainly attributed to a CNH bending vibration [14]. Dissolving the protein in D_2O, the deuterium atoms of the solvent exchange with the protein hydrogen atoms that are solvent accessible and the AII signal shifts at lower frequency, going from ca. 1550 cm^{-1} to ca. 1450 cm^{-1} (AII′) [14,40]. When the globular protein is folded, the hydrogen atoms located in the internal part of the structure are not exposed to the solvent and cannot exchange with deuterium atoms. Indeed, the FTIR spectra recorded at 20 °C have an intense AII′ band but still show the AII signal. With the temperature increasing, the protein tends to expose its hydrophobic portions and internal groups to the solvent, facilitating the H/D exchange [14]. In the spectra recorded at 95 °C the AII signal disappeared while the intensity of the AII′ band increased with respect the spectra recorded at 20 °C. The amide I (AI) band falls at 1650 cm^{-1} and is mostly ascribed to a CO stretching vibration of amide groups. The AI band is highly sensitive to the protein conformational changes because the amide carbonyl groups are directly involved in determining the protein secondary structure. Thus, by following the frequency position of the AI band, information on the protein conformational changes can be obtained. The β-Lg thermal unfolding is monitored recording the FTIR spectrum at each temperature in both heating and cooling scans, to verify the process reversibility. Fig. 1b reports the AI peak position as a function of temperature for the diluted protein solution. A sigmoidal-like curve is obtained with the largest variation appearing between 70 °C and 95 °C. This points out that the greatest conformational change takes place in this temperature range, as additionally supported by circular dichroism (CD) spectra reported in Fig. S2. In line with these findings, a structural rearrangement of the native β-Lg was found to occur at 80 °C and was attributed to the formation of a molten globule [41]. The process involves the loss of the tertiary structure and only a partial modification of the secondary one, with the formation of some disordered regions. The FTIR spectra recorded during the cooling scans highlight a good structural recovery of native β-Lg.

Increasing the β-Lg concentration up to 200 mg/mL, the system becames self-crowded, and the protein monomers can aggregate at high temperature, as testified by the strong increase of the component centred at 1617 cm^{-1} in the FTIR spectrum recorded at 95 °C (Fig. 1c). This component is diagnostic for protein aggregates with amyloid structure [40]. The absorbance changes observed at 1550 cm^{-1} (AII) and at 1617 cm^{-1} (amyloid aggregates) for the concentrated solution are reported in Fig. 1d. The full H/D exchange is reached at ca. 80 °C in proximity of the melting temperature estimated for the diluted sample; this indicates that the thermal-induced conformational change from the folded to the molten globule state, is not concentration-dependent. Overall, the occurrence of a cooperative two-state process, between the folded and partially unfolded (molten globule) species in thermal equilibrium can be conjectures [14]. In such a case, for temperatures close to the melting one, the increased fraction of the molten globule species, promotes the quick H/D exchange of the protein [14]. Fig. 1d also indicates that amyloid aggregation requires a fraction of molten globule species. Our finding remarks the idea that, in the case of β-Lg as for lysozyme [14], the formation of amyloid aggregates requires the exposition to the solvent of the proteins amyloidogenic portion. At the end of the heating cycle a transparent hydrogel is obtained at high temperature (inset of Fig. 1d). Results of FTIR measurements performed as a function of time in isothermal conditions (85 °C), reported in Fig. S4, clearly indicate that amyloid structures rapidly develop (within tens of minutes). Moreover, the system percolation is visually observed after 1 h of the isothermal cure at 85 °C for both samples (100 and 200 mg/mL). Comparing the thermal behaviour of β-Lg and lysozyme [14–16] in similar experimental conditions, i.e. similar concentration and pH, both globular proteins exhibit different unfolding mechanisms and different thermal stability of the formed amyloid aggregates. Indeed, the unfolding process of β-Lg passes through the molten globule intermediate state and the complete unfolding takes place at about 130 °C. Differently, lysozyme unfolding path can be described by a two-state model without intermediate species involvement, and the estimated melting temperature occurs at 53 °C [14–16]. The β-Lg molten globule in acidic conditions can form thermally stable amyloid aggregates that do not dissociate within the thermal range under consideration. These amyloid aggregates can reticulate directly at high temperature and the hydrogel phase is obtained. On the contrary, lysozyme amyloid oligomers are thermolabile and dissociate for temperature higher than 60 °C; in fact, the hydrogel forms at low temperatures, after the cooling back [14–16].

Fig. 2 reports the FTIR spectra as a function of temperature of the diluted and concentrated β-Lg solution at pH 7.5.

In Fig. 2b is reported the AI frequency position as a function of

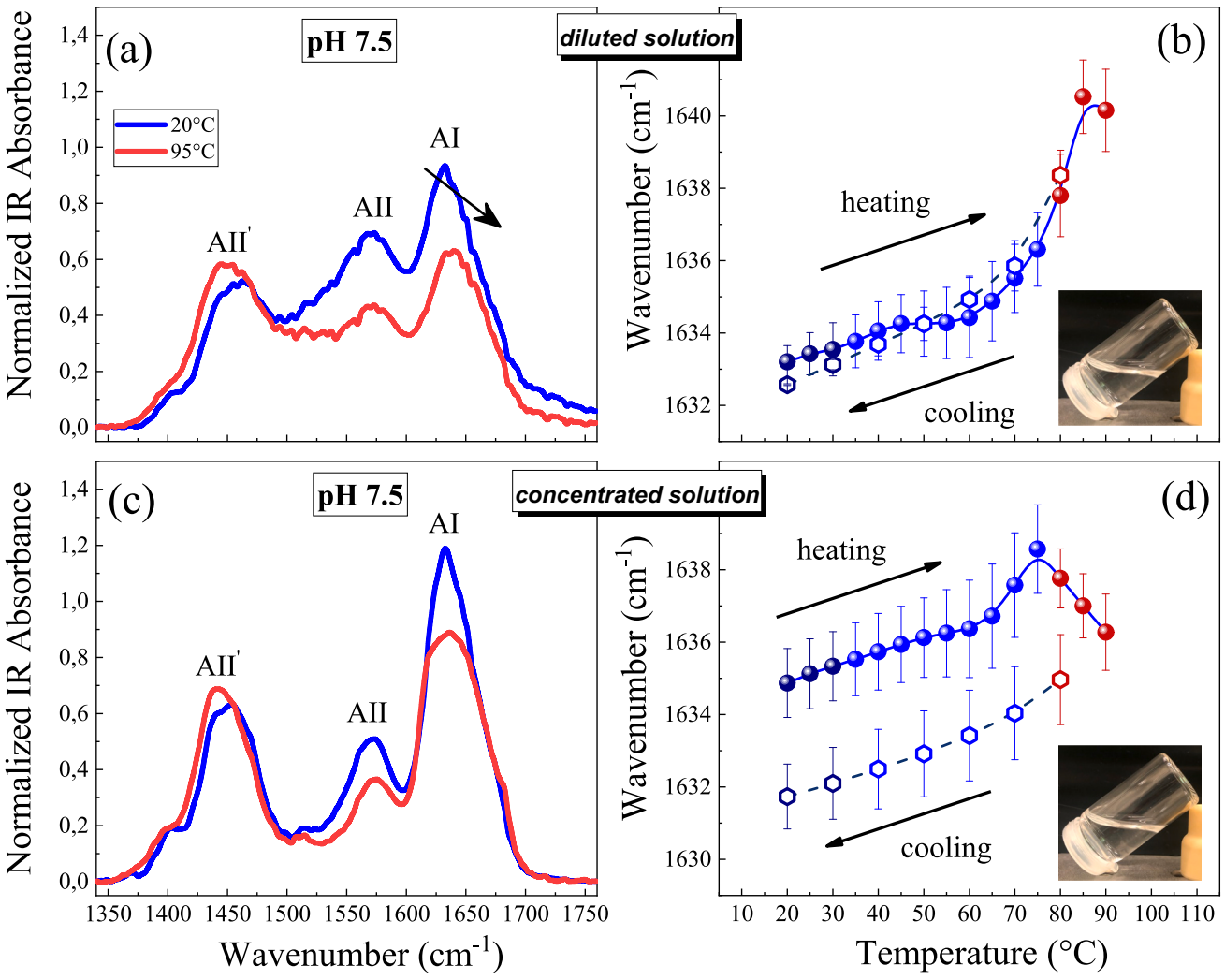

Fig. 2. Panels (a) and (c) show the FTIR spectra of β-Lg solutions at pH 7.5, recorded at 20 °C and at 95 °C, of the diluted (20 mg/mL) and of the concentrated (100 mg/ml) β-Lg solutions, respectively. Panels (b) and (d) report the temperature-dependence of the frequency centre of gravity of the AI signal during the heating and the cooling thermal treatments of the diluted and the concentrated β-Lg solutions, respectively. After the heating cycle the formation of gel is not observed even at protein concentrated conditions (see photo inside panel d).

temperature. The data trend highlights a strong variation of the β-Lg conformation from 70 °C to 95 °C as in the acidic conditions (Fig. 1b), also confirmed by CD experiments (Fig. S3). However, in a neutral environment the data show a smoother variation, suggesting a more gradual transition from the native to the molten globule state. The process is reversible as evidenced by the good superimposition of the heating and cooling curves. An important aspect to note from Fig. 2a,c is the behaviour of the AII band. In this case (neutral solution), unlike in the previous one (acid solution), the AII band does not disappear at 95 °C, despite the transition falls within the same range (70–95 °C). The persistence of the AII band at high temperatures suggests that some portions of β-Lg remain not accessible to the solvent, preventing the complete H/D substitution. Thus, the data indicate that the transition from the native to the molten globule state occurs at about 80 °C in both acidic and neutral conditions. Nevertheless, the molten globule conformation appears different at the two pH values. It can be conjectured that in acidic conditions, the molten globule has a more open structure, with the amyloidogenic portions more exposed to the solvent. As such, the system easily self-assembles at high concentrations to generate amyloid aggregates. On the contrary, in neutral conditions, the structure of the molten globule is relatively less opened, with modified aggregation propensity. In fact, in these conditions, the amyloid aggregates do not form and the sample gelation is not observed, even in very concentrated conditions. However, an overall broadening of the AI band is observed at increasing temperature (Fig. 2c), and the data trend of the cooling ramp (Fig. 2d) indicate some degree of irreversibility. These features can be explained considering that amorphous aggregation might partially take place in the concentrated sample at high temperatures. Overall, FTIR findings indicate that the formation of transparent gel in concentrated β-Lg solutions is related to the development of amyloid aggregates that, in turn, requires the presence of a specific molten globule conformation.

Comparing these results with those obtained previously with lysozyme, we observe a totally different behaviour of the melting temperature value as a function of the solution pH. In fact, the melting temperature of lysozyme is strongly dependent on the pH value, that moving from 4.5 to 1.8 strongly affects the lysozyme melting temperature reducing its value of about 20 °C [14]. Instead, as regards the transition temperature from the folded to the molten globule state, the stronger conformational variation of β-Lg always takes place between 70 °C and 85 °C. However, the molten globule intermediate states reached at acidic and at neutral conditions are different among them as asserted by the AII band thermal behaviour and by the totally different development of aggregation paths in the two experimental conditions.

3.2. β-Lg local conformation probed by UVRR spectroscopy

Resonance Raman spectroscopy allows to enhance those bands due to vibrational modes that are coupled to the selected electronic transition. Therefore, it provides specific information on the structure of proteins thanks to the sensitivity of the enhanced signals to the local chemical environment. Using excitation wavelength in the near UV (> 210 nm), the Raman spectrum of a protein is dominated by the signals coming from the phenol and the indole chromophores, which are the side groups of tyrosine and tryptophan amino acid residues, respectively. The absorption spectrum of tryptophan (Trp) and tyrosine (Tyr) at 226 nm, that is the used excitation wavelength of the present Raman experiments, derives from the $\pi - \pi^*$ electronic transition to the B_b state in Trp and L_a state in Tyr [42]. Consequently, a selective enhancement of Trp and Tyr bands occurs with negligible interference from amide bands and from bands associated with any other amino acid side chains.

The UVRR spectrum of β-Lg dissolved in D_2O (Fig. 3a) is dominated by the in-plane aromatic ring vibrations of Trp and Tyr, as supported by the spectra of Trp and Tyr solutions reported in Fig. 3b,c.

Tryptophan bands appear at 1018 cm^{-1} (Trp16), generated by the symmetric benzene/pyrrole out-of-phase breathing mode, at 1340–1360 cm^{-1} (Trp7), attributed to the Fermi resonance between N_1-C_8 stretching in pyrrole ring and combination bands of out-of-plane bending and at 1554 cm^{-1} (Trp3), related to the C_2-C_3 stretching mode of the pyrrole ring [42].

Tyrosine bands are observed at 1184 cm^{-1} (Tyr9a), generated by the in-plane C—H bending, at 1220 cm^{-1} (Tyr7a), related to the ring C-C_β stretching and at 1616 cm^{-1} (Tyr8a) due to the in-plane ring stretching [42].

The UV–Vis absorption band position and shape of Trp and Tyr is influenced by their surrounding chemical environment. In resonance conditions this effect modulates the Raman cross section and thus the intensity of the Raman bands of both aminoacidic residues. In proteins, the amino acid side-chain environment depends on several factors such as, the local packing of the neighbouring side chains, the contact with the backbone amide bonds, the exposure of the residue to the solvent and the interactions among protein monomers when aggregation or clustering occurs [43–45]. Therefore, in principle, it is possible to draw some conclusions concerning conformational rearrangements around the portions of the polypeptide chains where Trp and Tyr are located, by looking at the intensity variations of resonance Raman spectra recorded with 226 nm excitation.

Fig. 4a,b displays the UVRR spectra of the diluted and the concentrated β-Lg solutions at pH 1.4 collected at 22 °C (blue curves) and 85 °C (red curves). The intensity of the Trp Raman signals significantly varies when the temperature of the system is increased from 22 °C to 85 °C. The band that shows the greatest intensity variation is the Trp3 one. Fig. 4c

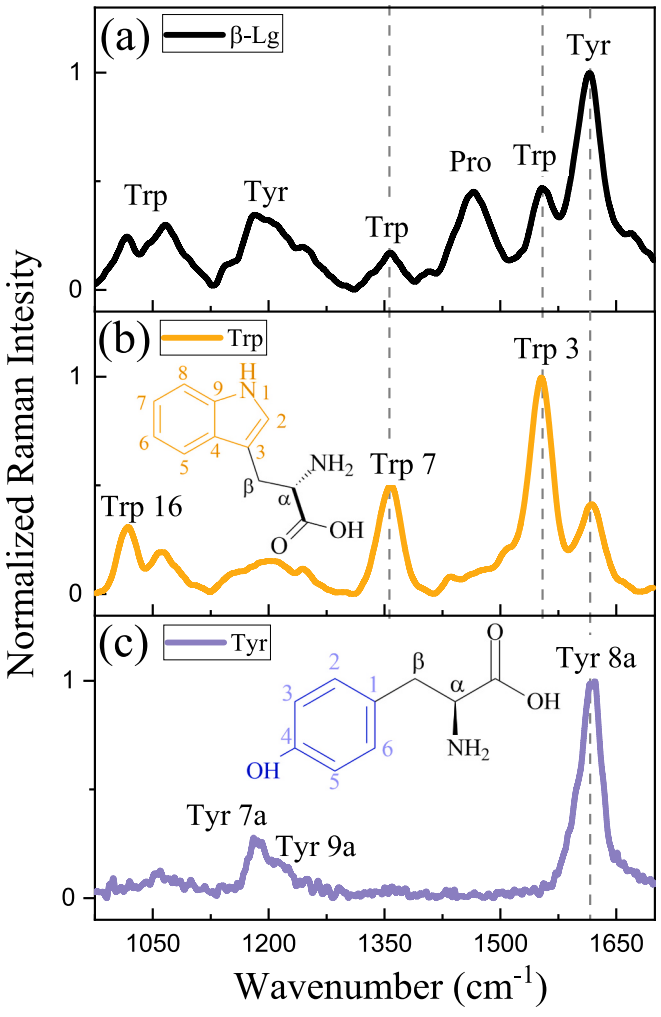

Fig. 3. UVRR spectra recorded with 226 nm excitation wavelength of (a) β-Lg, (b) tryptophan and (c) tyrosine dissolved in deuterium oxide at pH 1.4.

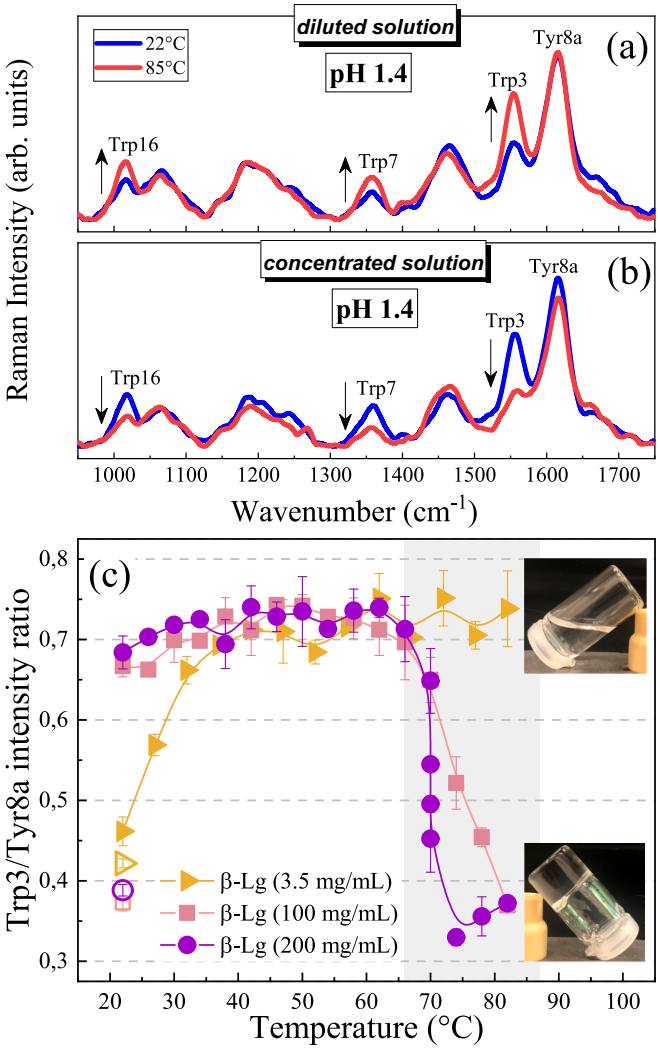

Fig. 4. UVRR spectra recorded at 22 °C and 85 °C with 226 nm excitation wavelength of (a) β-Lg 3.5 mg/mL and (b) β-Lg 100 mg/mL at pH 1.4. Panel (c) reports the Trp3/Tyr8a intensity ratio as a function of temperature estimated for diluted and concentrated solutions of β-Lg at pH 1.4. The empty symbols represent the cooling.

reports the Trp3/Tyr8a intensity ratio (I_{Trp}) for the investigated samples as a function of temperature in the 22–85 °C range and at 22 °C (empty symbols) after a fast-cooling back, performed to verify the reversibility of the process.

It is important to remark that the Raman signals related to Trp and Tyr are the result of the contribution of all the residues present in the β-Lg chain and it is not possible to discriminate among the different Trp and Tyr present in the structure [46]. As expected, the signal Tyr8a has a higher intensity compared to the Trp3 since the β-Lg contains four Tyr and two Trp residues [35,36]. The two Trp residues are located in different portions of the chain, one is into the protein hydrophobic core and the other is near the surface in an extremely mobile loop.

For the lower temperatures (<35 °C), I_{Trp} (see Fig. 4c) increases going from the diluted (3.5 mg/mL) to the concentrated (100 and 200 mg/mL) solutions. Considering that Trp(19) is buried into the β-barrel, it can be argued that a minor local rearrangement of the mobile loop where Trp(61) is located might take place upon concentration increase. In fact, the physical chemistry of self-crowded protein solutions becomes very complex. To describe their behaviour, it is necessary to consider additional parameters such as the interaction potential between proteins and both excluded volume and diffusive effects. Interestingly, for the diluted sample (3.5 mg/mL), I_{Trp} strongly increases with temperature in the 22–35 °C, becoming T-independent at T > 35 °C. This would suggest that the modifications involving the Trp(61) moiety occur at lower temperatures and that these are not connected with the extended global rearrangement, detected by FTIR and CD within 70–95 °C.

Concerning the concentrated samples, I_{Trp} is basically T-independent up to ca. 70 °C, showing a strong decrease (from 0.70 to 0.35) in the 70–85 °C range. This decrease occurs in the thermal range where the formation of amyloid aggregates takes place. These findings are consistent with previous UVRR studies on both lysozyme [47,48] and insulin fibrillation [49,50], where similarly the intensity damping of the UVRR signals of the aromatic residues was found to occur during amyloid aggregation. As a general explanation of the Trp Raman bands intensity variation, Asher and co-workers [51–53] suggest that this is related to the shift of the Trp absorption band, which depends on the involvement of the NH group of the indole ring in the formation of hydrogen bonds. When the NH group acts as H-donor, the electron density increases on the nitrogen atom and the energy of the HOMO molecular orbital rises up, causing the red shift of the absorption band and the enhancement of the Raman signal. On the contrary, when the NH acts as proton acceptor the heteroatom electron density decreases resulting in a stabilization of the HOMO energy level with a blue shift of the absorption band resulting in a decrement of the Raman signals intensity [51–53]. Thus, our experimental results highlight how the β-Lg amyloid aggregation also involves modifications of the local environment of Trp. This might include modulations of the H-bonding interactions formed by the Trp NH group either with other amino acid residues and/or with the solvent. The data corresponding to the cooling back of the systems in Fig. 4c provide evidence of a good recovery of the β-Lg structure in diluted conditions, when the aggregation does not occur, while confirming the persistence of amyloid aggregates in the concentrated solutions. The fact that I_{Trp} decreases upon formation of amyloid structures, is further confirmed by the UVRR spectra recorded at 85 °C as a function of time, shown in Fig. S5.

Fig. 5a,b reports the UVRR spectra of the diluted and the concentrated β-Lg solution at pH 7.5, while panel c reports the I_{Trp} obtained at different temperatures.

As observed for the acidic β-Lg solutions (Fig. 4c), the I_{Trp} obtained at 22 °C (Fig. 5c) increases passing from the diluted (3.5 mg/mL) to the concentrated (100 mg/mL) sample. As before, this might tentatively be ascribed to minor variations of the mobile loop, where Trp(61) is localized, upon concentration increase. The ratio does not depend on the protein amount starting from about 35 °C, showing similar trends in the whole temperature range. In particular, the I_{Trp} progressively increases with temperature above 60 °C, when major structural changes are

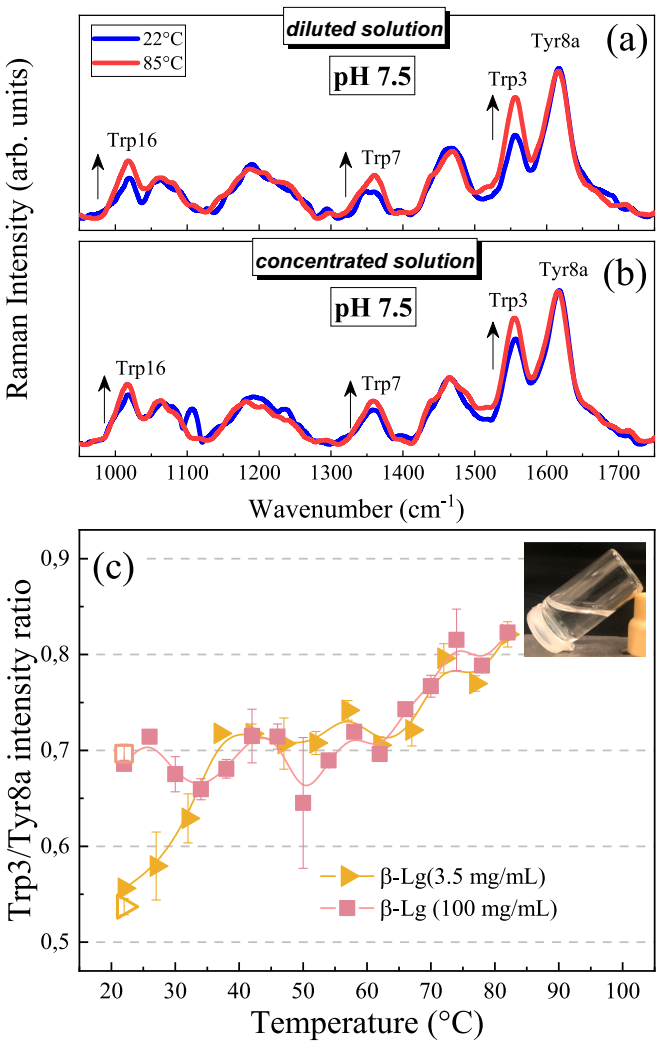

Fig. 5. UVRR spectra recorded at 22 °C and 85 °C with 226 nm excitation wavelength of (a) β-Lg 3.5 mg/mL and (b) β-Lg 100 mg/mL at pH 7.5. Panel (c) reports the Trp3/Tyr8a intensity ratio as a function of temperature estimated for diluted and concentrated solutions of β-Lg at pH 7.5. The empty symbols represent the cooling.

evidenced by FTIR spectra. Thus, at pH = 7.5 the transition from the folded to the molten globule state should involve modifications around the Trp residue. We remark that in the neutral conditions the thermal treatment does not lead to the formation of amyloid aggregates as in acidic conditions, when a substantial decrease of the I_{Trp} is observed. The cooling back of the systems (empty symbols in Fig. 5c) evidences a good recovery of the β-Lg structure at the two investigated protein concentrations, suggesting that the possible formation of amorphous aggregates is of minor importance and/or does not modify substantially the Trp environment.

The sketch of Fig. 6 summarizes the two different aggregation paths, i.e. amyloidogenic and non- amyloidogenic, occurring in concentrated solution of β-Lg protein during the heating of the sample. As mentioned above, the acid conditions lead to the formation of amyloidogenic aggregates that result in the transition from liquid to gel state for the concentrated solutions of β-Lg.

By combining the information obtained from the FTIR and UVRR spectra of the crowded samples we can schematize a different mechanism occurring in acidic and neutral conditions. Fig. 6A reports the structure of β-Lg in the folded state. Upon temperature increase, in a thermal range between 70 °C and 85 °C, the β-Lg starts to open leading to the molten globule state, as shown in Fig. 6B. The conformation

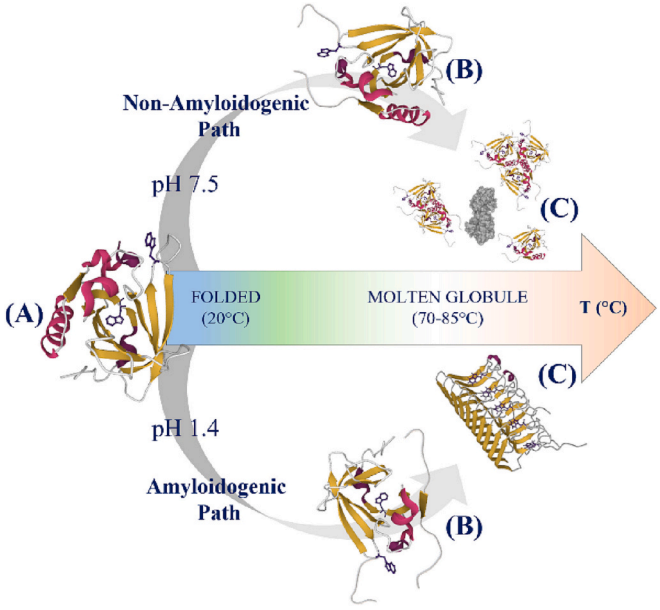

Fig. 6. Schematic representation of the thermally promoted aggregation paths of β-Lg at different pH conditions as detected by the joint in situ and operando FTIR and UVRR experiments.

assumed by the molten globule in acidic conditions is different from that in neutral conditions. Indeed, the molten globule conformation at neutral pH is not able to promote the amyloid aggregation route, probably weakly interacting clusters or some disordered aggregates can be formed. On the other hand, the molten globule conformation assumed by β-Lg at low pH is more open, triggering the amyloid aggregation, as pictured by Fig. 6C. The latter is spectroscopically identified through the growth of the FTIR signal at 1617 cm^{-1} which is peculiar to cross-β interaction and the drastic decrease of the Trp signal at 1554 cm^{-1} on the UVRR spectra. This suggests that the Trp located inside the β-barrel resides in the amylogenic portion (or very close to it), contributing to the stabilization of amyloid aggregates.

4. Conclusions

A general method, based on in situ FTIR and UVRR spectroscopy, is proposed here to shed light on the thermally-promoted aggregation behaviour of β-Lg as a function of the solution pH in a self-crowded milieu, for mimicking biomolecular dense packing in real natural systems [54]. Our experimental approach identifies specific IR and Raman spectroscopic markers that are strongly sensitive to both the β-Lg conformational changes and the self-aggregation mechanisms, in turn affected by the surrounding environment. Previous measurements on β-Lg conformational variation as a function of temperature, indicated the formation of a molten globule state at about 80 °C, identifying a second denaturation transition at 130 °C [55,56]. Here FTIR and UVRR spectra are recorded in the thermal range from 20 °C to 95 °C and thus the β-Lg transition from the folded to the molten globule state is followed *in real-time* conditions. As main achievement of our investigation, we can correlate specific IR and UVRR spectral changes to amyloidogenic or non-amyloidogenic aggregation pathways that the β-Lg protein experiences during the heating process. Our coherent view, obtained by matching the spectroscopic results coming from complementary non-destructive techniques, allows for revealing the existence of two different molten globule conformations able to select or not the amyloid aggregation route, as pictured in Fig. 6. These two different routes can be efficiently selected through the control of pH, i.e. the variation of β-Lg superficial charge. Indeed, the molten globule structure of β-Lg is less compact in acidic condition compared to the neutral one, even if the greatest conformational variation occurs in the same thermal range. A highly open conformation of β-Lg allows the exposition to the solvent of amyloidogenic portions, triggering the amyloid aggregation process that can occur only at low pH, when the formation of a transparent hydrogel is observed. The presence of amyloid aggregates is testified by the strong upturn of the marker signal in the medium IR region and by the greatest suppression of the I_{Trp} in the UVRR spectra occurring in the melting thermal range and in the self-crowded regime. The achievements of this work confirm the capability of the UVRR technique, in combination with conventional IR and CD experiments, to provide a local structural view on the complex macromolecular phenomena taking place during protein aggregation. Overall, results demonstrate that protein-based amyloid hydrogels can be quickly formed in self-crowding conditions at low pH. The formation of this type of amyloid hydrogel might be of relevance in cellular biology and in industrial sectors such as the pharmaceutical and food areas, when proteins denaturation occurs in concentrated systems. Amyloid-based hydrogels formed in crowded conditions can represent an interesting class of functional biomaterials and can be further exploited for studying aggregates networking. On this framework our future studies concern the understanding of proteins co-aggregation using the food proteins β-Lg and lysozyme together. Indeed, these two proteins are already amply used in food and pharmaceutical manufacture and might be employed as suitable model systems to investigate aggregate formation in crowded multicomponent samples. Multiprotein (amyloid) hydrogels could be developped to better control the biomaterial properties such as viscoelasticity, crucial for real applications.

Funding

This research was funded by Elettra Sincrotrone Trieste (proposal number 20205486), European Union's Horizon 2020 research, innovation program under grant agreement no 871124 Laserlab-Europe and the project CNR-FOE-LENS-2021, Ministero dell'Istruzione dell'Università e della Ricerca Italiano, PRIN2017-2017Z55KCW, Fondazione Cassa di Risparmio di Torino (Visco3DCell project), "E-REACT EU" the National Social Fund-National Operative Research Program and Innovation 2014-2020 (D.M. 1062/2021), personal Grant number 23-G-15445-3 (project "FSEREACT EU"), and by the European Union - NextGenerationEU under the Italian Ministry of University and Research (MUR) National Innovation Ecosystem grant ECS00000041 - VITALITY.

CRediT authorship contribution statement

Sara Venturi: Investigation, Writing – original draft, Writing – review & editing, Data curation. **Barbara Rossi:** Investigation, Resources, Writing – review & editing, Data curation, Supervision, Funding acquisition. **Mariagrazia Tortora:** Writing – review & editing. **Renato Torre:** Resources, Writing – review & editing, Funding acquisition. **Andrea Lapini:** Writing – review & editing. **Paolo Foggi:** Resources, Writing – review & editing, Funding acquisition. **Marco Paolantoni:** Writing – review & editing, Data curation, Visualization, Supervision. **Sara Catalini:** Conceptualization, Investigation, Resources, Writing – review & editing, Data curation, Visualization, Supervision, Project administration, Funding acquisition.

Declaration of competing interest

The authors declare that they have no known competing financial interests or personal relationships that could have appeared to influence the work reported in this paper.

Data availability

Data will be made available on request.

Acknowledgements

The authors acknowledge Elettra Sincrotrone Trieste for providing access to its synchrotron radiation facilities and for financial support (proposal number 20205486). The authors gratefully acknowledge A. Gessini for the technical support during the UVRR measurements at IUVS beamline of the Elettra Sincrotrone Trieste. A great acknowledgment event to European Union's Horizon 2020 research, the innovation program under grant agreement no 871124 Laserlab-Europe and Ministero dell'Istruzione dell'Università e della Ricerca Italiano, PRIN2017-2017Z55KCW for the financial support. MT thanks the European Regional Development Fund and Interreg V-A Italy Austria 2014–2020 through the Interreg Italy-Austria project ITAT 1059 InCIMa4 "InCIMa for Science and SMEs". S.C. thanks the research project "FSE-REACT EU" financed by National Social Fund-National Operative Research Program and Innovation 2014-2020 (D.M. 1062/2021), personal Grant number 23-G-15445-3. MP acknowledges Università degli Studi di Perugia and MUR for support within the project Vitality.

Appendix A. Supplementary data

Supplementary data to this article can be found online at https://doi.org/10.1016/j.ijbiomac.2023.124621.

References

[1] G. Faravelli, V. Mondani, P.P. Mangione, S. Raimondi, L. Marchese, F. Lavatelli, M. Stoppini, A. Corazza, D. Canetti, G. Verona, L. Obici, Amyloid formation by globular proteins: the need to narrow the gap between in vitro and in vivo mechanisms, Front. Mol. Biosci. 9 (2022) 100, https://doi.org/10.3389/fmolb.2022.830006.

[2] D.M. Fowler, A.V. Koulov, W.E. Balch, J.W. Kelly, Functional amyloid–from bacteria to humans, Trends Biochem. Sci. 32 (5) (2007) 217–224, https://doi.org/10.1016/j.tibs.2007.03.003.

[3] J. Li, F. Zhang, Amyloids as building blocks for macroscopic functional materials: designs, applications and challenges, Int. J. Mol. Sci. 22 (19) (2021) 10698, https://doi.org/10.3390/ijms221910698.

[4] D. Li, E.M. Jones, M.R. Sawaya, H. Furukawa, F. Luo, M. Ivanova, S.A. Sievers, W. Wang, O.M. Yaghi, C. Liu, D.S. Eisenberg, Structure-based design of functional amyloid materials, J. Am. Chem. Soc. 136 (52) (2014) 18044–18051, https://doi.org/10.1021/ja509648u.

[5] T.P. Knowles, R. Mezzenga, Amyloid fibrils as building blocks for natural and artificial functional materials, Adv. Mater. 28 (31) (2016) 6546–6561, https://doi.org/10.1002/adma.20150596.

[6] G. Wei, Z. Su, N.P. Reynolds, P. Arosio, I.W. Hamley, E. Gazit, R. Mezzenga, Self-assembling peptide and protein amyloids: from structure to tailored function in nanotechnology, Chem. Soc. Rev. 46 (15) (2017) 4661–4708, https://doi.org/10.1039/C6CS00542J.

[7] Jansen, et al., Rational Design of Amyloid-like Fibrillary Structures, Compr. Rev. Food Sci. Food Saf. 18 (1) (2019) 84–105, https://doi.org/10.1111/1541-4337.12404.

[8] Keppler, Protein oxidation during temperature-induced, Food Chemistry 289 (2019) 223–231, https://doi.org/10.1016/j.foodchem.2019.02.114.

[9] W.S. Gosal, A.H. Clark, P.D. Pudney, S.B. Ross-Murphy, Novel amyloid fibrillar networks derived from a globular protein: β-lactoglobulin, Langmuir 18 (19) (2002) 7174–7181, https://doi.org/10.1021/la025531a.

[10] N. Harn, C. Allan, C. Oliver, C.R. Middaugh, Highly concentrated monoclonal antibody solutions: direct analysis of physical structure and thermal stability, J. Pharm. Sci. 96 (3) (2007) 532–546, https://doi.org/10.1002/jps.20753.

[11] G. Rivas, A.P. Minton, Macromolecular crowding in vitro, in vivo, and in between, Trends Biochem. Sci. 41 (11) (2016) 970–981, https://doi.org/10.1016/j.tibs.2016.08.013.

[12] B. Ma, et al., Macromolecular crowding modulates the kinetics and morphology of amyloid self-assembly by β-lactoglobulin, Int. J. Biol. Macromol. 53 (2013) 82–87, https://doi.org/10.1016/j.ijbiomac.2012.11.008.

[13] J.T. King, et al., Crowding induced collective hydration of biological macromolecules over extended distances, J. Am. Chem. Soc. 136 (1) (2014) 188–194, https://doi.org/10.1021/ja407858c.

[14] S. Catalini, D.R. Perinelli, P. Sassi, L. Comez, G.F. Palmieri, A. Morresi, G. Bonacucina, P. Foggi, S. Pucciarelli, M. Paolantoni, Amyloid self-assembly of lysozyme in self-crowded conditions: the formation of a protein oligomer hydrogel, Biomacromolecules 22 (3) (2021) 1147–1158, https://doi.org/10.1021/acs.biomac.0c01652.

[15] S. Catalini, A. Taschin, P. Bartolini, P. Foggi, R. Torre, Probing globular protein self-assembling dynamics by heterodyne transient grating experiments, Appl. Sci. 9 (3) (2019) 405, https://doi.org/10.3390/app9030405.

[16] S. Catalini, V. Lutz-Bueno, M. Usuelli, M. Diener, A. Taschin, P. Bartolini, P. Foggi, M. Paolantoni, R. Mezzenga, R. Torre, Multi-length scale structural investigation of lysozyme self-assembly, Iscience 25 (7) (2022), 104586, https://doi.org/10.1016/j.isci.2022.104586.

[17] T. Miti, M. Mulaj, J.D. Schmit, M. Muschol, Stable, metastable, and kinetically trapped amyloid aggregate phases, Biomacromolecules 16 (1) (2015) 326–335, https://doi.org/10.1021/bm501521r.

[18] F. Hasecke, T. Miti, C. Perez, J. Barton, D. Schölzel, L. Gremer, C.S. Grüning, G. Matthews, G. Meisl, T.P. Knowles, D. Willbold, Origin of metastable oligomers and their effects on amyloid fibril self-assembly, Chem. Sci. 9 (27) (2018) 5937–5948, https://doi.org/10.1039/C8SC01479E.

[19] D. Kurouski, R.P. Van Duyne, I.K. Lednev, Exploring the structure and formation mechanism of amyloid fibrils by Raman spectroscopy: a review, Analyst 140 (15) (2015) 4967–4980, https://doi.org/10.1039/C5AN00342C.

[20] Y. Cao, J. Adamcik, M. Diener, J.R. Kumita, R. Mezzenga, Different folding states from the same protein sequence determine reversible vs irreversible amyloid fate, J. Am. Chem. Soc. 143 (30) (2021) 11473–11481, https://doi.org/10.1021/jacs.1c03392.

[21] R. Carrotta, R. Bauer, R. Waninge, C. Rischel, Conformational characterization of oligomeric intermediates and aggregates in β-lactoglobulin heat aggregation, Protein Sci. 10 (7) (2001) 1312–1318, https://doi.org/10.1110/ps.42501.

[22] Y. Shen, et al., From protein building blocks to functional materials, ACS Nano 15 (4) (2021) 5819–5837, https://doi.org/10.1021/acsnano.0c08510.

[23] S.R. Euston, S. Ur-Rehman, G. Costello, Denaturation and aggregation of β-lactoglobulin a preliminary molecular dynamics study, Food Hydrocoll. 21 (7) (2007) 1081–1091, https://doi.org/10.1016/j.foodhyd.2006.07.018.

[24] D. Stanić-Vučinić, T. Ćirković-Veličković, The modifications of bovine beta-lactoglobulin-effects on its structural and functional properties, Journal of the Serbian Chemical Society 78 (3) (2013) 445–461, https://doi.org/10.2298/JSC120810155S.

[25] K. Broersen, Milk processing affects structure, bioavailability and immunogenicity of β-lactoglobulin, Foods 9 (7) (2020) 874, https://doi.org/10.3390/foods9070874.

[26] Z. Teng, R. Xu, Q. Wang, Beta-lactoglobulin-based encapsulating systems as emerging bioavailability enhancers for nutraceuticals: a review, RSC Adv. 5 (44) (2015) 35138–35154, https://doi.org/10.1039/C5RA01814E.

[27] C. Li, J. Adamcik, R. Mezzenga, Biodegradable nanocomposites of amyloid fibrils and graphene with shape-memory and enzyme-sensing properties, Nat. Nanotechnol. 7 (7) (2012) 421–427. https://www.nature.com/articles/nnano.2012.62.

[28] Y. Han, Y. Cao, S. Bolisetty, T. Tian, S. Handschin, C. Lu, R. Mezzenga, Amyloid fibril-templated high-performance conductive aerogels with sensing properties, Small 16 (45) (2020) 2004932, https://doi.org/10.1002/smll.202004932.

[29] T. Jin, M. Peydayesh, H. Joerss, J. Zhou, S. Bolisetty, R. Mezzenga, Amyloid fibril-based membranes for PFAS removal from water, Environ. Sci.: Water Res. Technol. 7 (10) (2021) 1873–1884, https://doi.org/10.1039/D1EW00373A.

[30] M. Peydayesh, M.K. Suter, S. Bolisetty, S. Boulos, S. Handschin, L. Nyström, R. Mezzenga, Amyloid fibrils aerogel for sustainable removal of organic contaminants from water, Adv. Mater. 32 (12) (2020) 1907932, https://doi.org/10.1002/adma.201907932.

[31] W.S. Gosal, A.H. Clark, S.B. Ross-Murphy, Fibrillar β-lactoglobulin gels: Part 1. Fibril formation and structure, Biomacromolecules 5 (6) (2004) 2408–2419, https://doi.org/10.1021/bm049659d.

[32] M.Z. Papiz, L. Sawyer, E.E. Eliopoulos, A.C.T. North, J.B.C. Findlay, R. Sivaprasadarao, T.A. Jones, M.E. Newcomer, P.J. Kraulis, The structure of β-lactoglobulin and its similarity to plasma retinol-binding protein, Nature 324 (6095) (1986) 383–385. https://www.nature.com/articles/324383a0.

[33] K. Kuwata, M. Hoshino, V. Forge, S. Era, C.A. Batt, Y. Goto, Solution structure and dynamics of bovine β-lactoglobulin A, Protein Sci. 8 (11) (1999) 2541–2545, https://doi.org/10.1110/ps.8.11.2541.

[34] G. Kontopidis, C. Holt, L. Sawyer, Invited review: β-lactoglobulin: binding properties, structure, and function, J. Dairy Sci. 87 (4) (2004) 785–796, https://doi.org/10.3168/jds.S0022-0302(04)73222-1.

[35] S. Brownlow, J.H.M. Cabral, R. Cooper, D.R. Flower, S.J. Yewdall, I. Polikarpov, A. C. North, L. Sawyer, Bovine β-lactoglobulin at 1.8 Å resolution still an enigmatic lipocalin, Structure 5 (4) (1997) 481–495, https://doi.org/10.1016/S0969-2126(97)00205-0.

[36] V. Vetri, V. Militello, Thermal induced conformational changes involved in the aggregation pathways of beta-lactoglobulin, Biophys. Chem. 113 (1) (2005) 83–91, https://doi.org/10.1016/j.bpc.2004.07.042.

[37] B. Rossi, C. Bottari, S. Catalini, F. D'Amico, A. Gessini, C. Masciovecchio, Synchrotron-based ultraviolet resonance Raman scattering for material science, in: Molecular and Laser Spectroscopy, Elsevier, 2020, pp. 447–482, https://doi.org/10.1016/b978-0-12-818870-5.00013-7.

[38] B. Rossi, M. Tortora, S. Catalini, A. Gessini, C. Masciovecchio, in: Synchrotron-based UV Resonance Raman Spectroscopy for Polymer Characterization. Spectroscopic Techniques for Polymer Characterization: Methods, Instrumentation, Applications, 2021, pp. 183–225, https://doi.org/10.1002/9783527830312.ch7.

[39] L. Comez, et al., Heat-induced self-assembling of BSA at the isoelectric point, Int. J. Biol. Macromol. 177 (2021) 40–47, https://doi.org/10.1016/j.ijbiomac.2021.02.112.

[40] A. Barth, Infrared spectroscopy of proteins, Biochim. Biophys. Acta Bioenerg. 1767 (9) (2007) 1073–1101, https://doi.org/10.1016/j.bbabio.2007.06.004.

[41] Y. Fang, D.G. Dalgleish, Conformation of β-lactoglobulin studied by FTIR: effect of pH, temperature, and adsorption to the oil–water interface, J. Colloid Interface Sci. 196 (2) (1997) 292–298, https://doi.org/10.1006/jcis.1997.5191.

[42] N. Cho, S. Song, S.A. Asher, UV resonance Raman and excited-state relaxation rate studies of hemoglobin, Biochemistry 33 (19) (1994) 5932–5941, https://doi.org/10.1021/bi00185a034.
[43] B. Rossi, S. Catalini, C. Bottari, A. Gessini, C. Masciovecchio, Frontiers of UV resonant raman spectroscopy by using synchrotron radiation: The case of aqueous solvation of model peptides, in: UV and Higher Energy Photonics: From Materials to Applications 11086, 2019, pp. 23–32, https://doi.org/10.1117/12.2529172.
[44] S. Catalini, B. Rossi, P. Foggi, C. Masciovecchio, F. Bruni, Aqueous solvation of glutathione probed by UV resonance Raman spectroscopy, J. Mol. Liq. 283 (2019) 537–547, https://doi.org/10.1016/j.molliq.2019.03.113.
[45] S. Catalini, B. Rossi, M. Tortora, P. Foggi, A. Gessini, C. Masciovecchio, F. Bruni, Hydrogen bonding and solvation of a proline-based peptide model in salt solutions, Life 11 (8) (2021) 824, https://doi.org/10.3390/life11080824.
[46] H. Takeuchi, UV raman markers for structural analysis of aromatic side chains in proteins, Anal. Sci. 27 (11) (2011) 1077, https://doi.org/10.2116/analsci.27.1077.
[47] M. Xu, V.V. Ermolenkov, V.N. Uversky, I.K. Lednev, Hen egg white lysozyme fibrillation: a deep-UV resonance raman spectroscopic study, J. Biophotonics 1 (3) (2008) 215–229, https://doi.org/10.1002/jbio.200710013.
[48] M. Pachetti, F. D'Amico, L. Pascolo, S. Pucciarelli, A. Gessini, P. Parisse, L. Vaccari, C. Masciovecchio, UV resonance raman explores protein structural modification upon fibrillation and ligand interaction, Biophys. J. 120 (20) (2021) 4575–4589, https://doi.org/10.1016/j.bpj.2021.08.032.
[49] D. Kurouski, J. Washington, M. Ozbil, R. Prabhakar, A. Shekhtman, I.K. Lednev, Disulfide bridges remain intact while native insulin converts into amyloid fibrils, PLoS One 7 (6) (2012), e36989, https://doi.org/10.1371/journal.pone.0036989.
[50] D. Kurouski, T. Deckert-Gaudig, V. Deckert, I.K. Lednev, Structure and composition of insulin fibril surfaces probed by TERS, J. Am. Chem. Soc. 134 (32) (2012) 13323–13329, https://doi.org/10.1021/ja303263y.
[51] Z. Chi, S.A. Asher, UV Raman determination of the environment and solvent exposure of Tyr and Trp residues, J. Phys. Chem. B 102 (47) (1998) 9595–9602, https://doi.org/10.1021/jp9828336.
[52] Z. Ahmed, I.A. Beta, A.V. Mikhonin, S.A. Asher, UV− resonance Raman thermal unfolding study of Trp-cage shows that it is not a simple two-state miniprotein, J. Am. Chem. Soc. 127 (31) (2005) 10943–10950, https://doi.org/10.1021/ja050664e.
[53] Z. Chi, S.A. Asher, Ultraviolet resonance Raman examination of horse apomyoglobin acid unfolding intermediates, Biochemistry 38 (26) (1999) 8196–8203, https://doi.org/10.1021/bi982654e.
[54] I.M. Kuznetsova, K.K. Turoverov, V.N. Uversky, What macromolecular crowding can do to a protein, Int. J. Mol. Sci. 15 (12) (2014) 23090–23140, https://doi.org/10.3390/ijms151223090.
[55] M.A. Hoffmann, P.J. van Mil, Heat-induced aggregation of β-lactoglobulin as a function of pH, J. Agric. Food Chem. 47 (5) (1999) 1898–1905, https://doi.org/10.1021/jf980886e.
[56] S. Le Maux, S. Bouhallab, L. Giblin, A. Brodkorb, T. Croguennec, Bovine β-lactoglobulin/fatty acid complexes: binding, structural, and biological properties, Dairy Sci. Technol. 94 (5) (2014) 409–426, https://doi.org/10.1007/s13594-014-0160-y.